N O T I C E

THIS DOCUMENT HAS BEEN REPRODUCED FROM
MICROFICHE. ALTHOUGH IT IS RECOGNIZED THAT
CERTAIN PORTIONS ARE ILLEGIBLE, IT IS BEING RELEASED
IN THE INTEREST OF MAKING AVAILABLE AS MUCH
INFORMATION AS POSSIBLE

Efficiency of Aerosol Collection on Wires Exposed in the Stratosphere

Homer Y. Lem and Neil H. Farlow

October 1979

NASA

National Aeronautics and
Space Administration

Efficiency of Aerosol Collection on Wires Exposed in the Stratosphere

Homer Y. Lem, LFE Environmental Analysis Laboratories, Richmond, California
Neil H. Farlow, Ames Research Center, Moffett Field, California

EFFICIENCY OF AEROSOL COLLECTION ON WIRES
EXPOSED IN THE STRATOSPHERE

Homer Y. Lem
LFE Environmental Analysis Laboratories

and

Neil H. Farlow
Ames Research Center

SUMMARY

The theory of inertial impaction is briefly presented; by and large the calibration experiments of Wong et al. (ref. 13) confirm the theoretical calculations.

In many respects the stratospheric aerosol research experiments performed at Ames Research Center are virtual duplications of the Wong et al. experiments, except for the pressure effect that can be corrected by using the Stokes-Cunningham slip factor. Consequently, the use of the curve of inertial paramenters vs particle collection efficiency, derived from Wong et al., is justified. The results show that stratospheric aerosol particles of all sizes are collectible by our wire impaction technique. Curves and tables are presented and used to correct particle counts for collection efficiencies less than 100%.

INTRODUCTION

The Atmospheric Experiments Branch at Ames Research Center has conducted an ongoing aerosol study in the lower stratosphere for many years. Special aerosol collecting devices are being flown on NASA U-2 aircraft at altitudes from 12 km to 21 km (ref. 1). Cylindrical wires of various sizes for particle-size-distribution studies and special thin films supported by electron grids for chemical and physical studies are used as collecting surfaces. The particle-size distributions and the chemical and physical studies have been discussed in many papers (refs. 2-6). To interpret the particle-size distribution results, theoretical calculations of aerosol collection efficiency and calibration experiments are needed. In fulfillment of one of these needs, this paper reviews and discusses aerosol collection theory and the application of the theory to our existing wire collection method at stratospheric conditions.

The individual thin wires we use for our aerosol collections can be considered, from a theoretical point of view, as basic elements in a filter. As particle-laden air approaches a cylindrical element, air molecules flow around it, while the particles tend, by inertia, to follow straighter paths that may intersect the cylinder, resulting in the particles being collected. The interaction of air molecules trying to drag the particles along airflow

1

lines and inertial effects tending to make the particles travel straight paths results in modified particle trajectories that may or may not intersect the collector. The size and mass of the particles, the properties of the air, and the collector size and configuration all, of course, influence whether the particle will follow a straighter path (and hit the cylinder) or a more curved path (and miss the cylinder). When a particle, initially on a trajectory that should intersect the cylinder, is moved by the diverging airflow to miss the target, then there is a collection efficiency problem. Understanding and correcting for this problem is the purpose of this paper.

BACKGROUND

Theoretical studies of particle collection by filtration were made as early as 1931 by Sell (ref. 7) and Albrecht (ref. 8). During World War II, Langmuir and Blodgett (ref. 9) systematically studied the theory of filtration by isolating a fiber in an ideal airflow. Shortly after Langmuir and Blodgett's work, Landahl and Herrmann (ref. 10) published some of their theoretical calculations on particles collected by impaction with moderate airflows at a Reynolds number (Re_f) of 10. Davies (ref. 11) also calculated collection efficiency, but in a viscous flow at $Re_f = 0.2$. Because results of the theoretical studies by the above authors were not in total agreement, Ranz and Wong (ref. 12) tried to verify the theory experimentally, with some success. Later, Wong et al. (ref. 13) completed another accurately calibrated experiment with different sizes of cylinders in a further verification of the theory, including the effect on collection efficiency of sampling at different Reynolds numbers. Generally, the various experimental results are in good agreement with the theory at high Reynolds number, but there is no reliable experimental data for low Reynolds numbers in viscous flow.

The efficiency with which aerosol particles are collected on an isolated cylinder is influenced by particle inertial impaction, direct interception, Brownian diffusion, gravity settling, and electrical and thermal effects. All of these mechanisms, except particle inertial impaction, are found to be insignificant under our collection conditions (see appendix). Consequently, the following discussions are limited to inertial impaction theory only.

Before we untangle the mathematical analysis of the theory, let us review the basic concept of filtration — mainly the mechanical (momentum) transport process in the gas-particle system (ref. 14) and in the gas-obstacle system (ref. 15) that determines whether a particle will miss the cylinder or be collected by it. We define the gas-particle system to be air-intermixed with aerosol particles, and the gas-obstacle system to be air-containing the collection cylinder.

In the gas-particle system, two dimensionless parameters (of many) are important enough to warrant detailed discussion. First to be considered is the Knudsen number, which provides a measure of the departure of the transport process from the laws of continuum mechanics. The definition of Knudsen number (K_{n_i}) for a particle of radius R_i in an infinite gas medium is

$$K_{n_i} = \frac{\lambda_g}{R_i} \quad \text{for} \quad 0 < K_{n_i} < \infty \tag{1}$$

where λ_g is the mean free path of the gas molecules. Over the range 0 to ∞, K_{n_i} is divided into four regions, each region being assigned an arbitrary value.

1. The continuum region, $K_{n_i} \to 0$ — The motion of the gas molecules in the vicinity of the particle is dominated by collisions, and all of the transfer processes of the gas molecules to and from the particle are of a diffusive character. Such a gas can be regarded as a continuum medium and the transport process as a continuum process. Any finite Knudsen number >0 is regarded as in the noncontinuum regime.

2. The slip-flow region, $0 < K_{n_i} < 0.25$ — In this region the transfer processes are described by applying a correction factor to the continuum.

3. The transition region, $0.25 < K_{n_i} < 10$ — At present there is only an inexact theory to describe the transfer processes in this region; there are difficulties in describing the molecular motion and in obtaining accurate experimental data (ref. 14).

4. The free-molecular region, $K_{n_i} > 10$ — There are no intermolecular collisions between gas molecules near the particle, and the gas molecules travel in straight-line paths. The particle may also be considered as a large molecule undergoing independent and binary collisions with the gas molecules.

In the upper tropopause and lower stratosphere, the transport processes for aerosol particles are in the transition region.

The second dimensionless parameter to be considered in the gas-particle system is the Reynolds number of a particle moving steadily through a stagnant medium of infinite extent. The Reynolds number of a particle in this flow field is

$$Re_i = \frac{2\rho_g R_i |(u - v)|}{\mu_g} \tag{2}$$

where ρ_g = gas density, u = particle velocity, v = gas velocity, and μ_g = gas viscosity. When $Re_i < 0.1$ and when the gas inertia is minimal, the Stokes-Cunningham resistance law gives a good approximation of particle motion. When $Re_i > 0.1$ or when the gas inertia becomes significant, the calculation of particle motion is extremely complex. For our sampling situation in the upper troposphere and lower stratosphere, we apply the Stokes-Cunningham resistance law.

3

In the gas-obstacle system, the same two dimensionless parameters are important. In this system, the Knudsen number is

$$K_{n_i} = \frac{\lambda_g}{R_c} \qquad \text{for} \quad 0 < K_{n_i} < \infty \tag{3}$$

where R_c is the collector radius. All of the transport processes in the gas-obstacle system are described in much the same way as in the gas-particle system. But now the transport processes are in the continuum region in our sampling situation.

The Reynolds number of flow in the gas-obstacle system is

$$Re_f = \frac{2\rho_g R_c v}{\mu_g} \qquad \text{for} \quad 0 < Re_f < \infty \tag{4}$$

where R_c = obstacle radius. When the gas is frictionless, incompressible, and $Re_f \rightarrow \infty$, and when the flow is irrotational, a potential flow field in the high Reynolds number region is defined; when $Re_f \rightarrow 0$, a viscous flow field exists. Our sampling conditions are between these two extreme flow regions for the gas-obstacle system. More detailed discussion of flow conditions will be presented in a later section.

Having reviewed the transport processes affecting the particles, we can now proceed with the mathematical analysis of the theory. With the restrictions in mind for our sampling situation for the two dimensionless parameters in the gas-particle system and the gas-obstacle system, consider a gas laden with aerosol particles moving toward a circular cylinder placed perpendicular to the direction of flow (fig. 1). As the gas is deflected around the cylinder, a particle moving with the gas tends to cross the streamlines and impact on the surface of the cylinder. As we said before, two effects influence the particle movement: inertia that tends to make the particle follow a straight path, and frictional drag forces that tend to slow the particle motion relative to the gas stream and divert the particle from its initial trajectory. This frictional drag force opposing the particle motion is

$$D^c = -6\pi\mu_g R_i (u - v) \tag{5}$$

where u = particle velocity and v = gas velocity, or

$$D^c = -\frac{(u - v)}{B_i} \tag{6}$$

where $B_i = 1/6\pi\mu_g R_i$ and $Re_i \ll 0.1$. Mobility (B_i) (ref. 14) is defined as a proportionality constant of the ratio of the velocity of a particle to the force acting on the particle. But the mobility of a particle depends on the value of $K_{n_i} = \lambda_g/R_i$. When this Knudsen number becomes finite, such as in

4

the transition region where we sample and in the free molecule region, the mobility relation must be corrected empirically by

$$B_i = \frac{(1 + \tilde{A}K_{n_i})}{6\pi\mu_g R_i} \qquad (7)$$

where $\tilde{A}$ is a constant. The coefficient $1 + \tilde{A}K_{n_i}$ is called the Stokes-Cunningham correction. Furthermore, $\tilde{A} = \hat{A} + \hat{B} \exp(1 - \hat{C}/K_{n_i})$, where $\hat{A}$, $\hat{B}$, and $\hat{C}$ are constants (ref. 14).

Introducing values for all of these coefficients in our sampling situation, $\tilde{A} = 1.23 + 0.41 \exp(-0.44 \, D_p/\lambda_g)$, and

$$B_i = \frac{1}{6\pi\mu_g R_i} \left\{ 1 + \frac{\lambda_g}{D_p} \left[1.23 + 0.41 \exp\left(\frac{-0.44 \, D_p}{\lambda_g}\right) \right] \right\} \qquad (8)$$

we can solve for B_i where D_p = particle diameter. This result, then, represents particle mobility due to drag on the particle by the diverging airstream.

Now, if all the forces other than the frictional drag are inactive, Newton's law of motion can be applied to the movement of the particle as follows:

$$M \frac{du}{dt} = - \frac{(u - v)}{B_i} \qquad (9)$$

provided that $0 \leqslant K_{n_i} \leqslant \infty$, $Re_i < 0.1$, and M = particle mass.

Again, u is the particle velocity and v is the gas velocity. Substituting and solving,

$$\frac{4}{3} \pi R_i^3 \rho_i \frac{du}{dt} = - \frac{6\pi\mu_g R_i}{C_c} (u - v)$$

where C_c is Stokes-Cunningham correction, ρ_i is particle density, and $R_i = D_p/2$:

$$\frac{1}{18} \frac{C_c \rho_i D_p^2}{\mu_g} \frac{du}{dt} + u - v = 0 \qquad (10)$$

In Cartesian coordinate forms, the equations reduce to

$$\frac{1}{18} \frac{C_c \rho_i D_p^2}{\mu_g} \frac{d^2 x}{dt^2} + \frac{dx}{dt} - v_x = 0 \qquad x,y = \text{position coordinates} \quad (11)$$

5

and

$$\frac{1}{18} \frac{C_c \rho_1 D_p^2}{\mu_g} \frac{d^2 y}{dt^2} + \frac{dy}{dt} - v_y = 0 \qquad (12)$$

To solve these two equations, we convert them into dimensionless forms with the following dimensionless parameters: $\bar{t} = 2vt/D_c$; $\bar{u}_x = u_x/v$; $\bar{u}_y = u_y/v$; $\bar{x} = 2x/L_c$; $\bar{y} = 2y/D_c$; $\bar{v}_x = v_x/v$; $\bar{v}_y = v_y/v$; $\bar{y}_o =$ original y position of particle at $\bar{t} = 0$; and $\bar{y}^* = \bar{y}_o$ position of the particle where its trajectory is tangent to the cylinder (see fig. 1). Defining terms, $x, y =$ position coordinates; $v =$ the gas velocity at a large distance from cylinder; $t =$ time; and $D_c =$ the cylinder diameter. Substituting these dimensionless parameters into the equations,

$$\frac{C_c \rho_1 D_p^2}{18 \mu_g} \frac{(D_c/2) d^2 \bar{x}}{(D_c^2/4v^2) d\bar{t}^2} + \frac{(D_c/2) d\bar{x}}{(D_c/2v) d\bar{t}} - v \bar{v}_x = 0 \qquad (13)$$

$$\left(\frac{C_c \rho_1 D_p^2}{18 \mu_g} \right) \left(\frac{2v^2}{D_c} \right) \frac{d^2 \bar{x}}{d\bar{t}^2} + v \frac{d\bar{x}}{d\bar{t}} - v \bar{v}_x = 0 \qquad (14)$$

$$v \left(2\psi \frac{d^2 \bar{x}}{d\bar{t}^2} + \frac{d\bar{x}}{d\bar{t}} - \bar{v}_x \right) = 0 \qquad (15)$$

where

$$\psi = \frac{C_c \rho_1 D_p^2 v}{18 \mu_g D_c}$$

and

$$2\psi \frac{d^2 \bar{x}}{d\bar{t}^2} + \frac{d\bar{x}}{d\bar{t}} - \bar{v}_x = 0 \qquad (16)$$

Similarly,

$$2\psi \frac{d^2 \bar{y}}{d\bar{t}^2} + \frac{d\bar{y}}{d\bar{t}} - \bar{v}_y = 0 \qquad (17)$$

Wong et al. (ref. 13) explained the meaning of the inertial parameter ψ and the collection efficiency as follows:

> The inertial parameter ψ has a physical significance in that it is the ratio of the stopping distance, i.e., the particle will travel in still air when given an initial velocity of v_o, to the diameter of the cylinder. $\bar{v}_x$ and $\bar{v}_y$ are the components of gas velocity which are related to the position $\bar{x}$ and $\bar{y}$, and the Reynolds number of flow across the cylinder. When $\bar{t} = 0$, and $\bar{x} = -\infty$, the boundary conditions will be $\bar{y} = \bar{y}_o$, $d\bar{x}/d\bar{t} = 1$, and $d\bar{y}/d\bar{t} = 0$.

6

And for a given particle and flow conditions, the above equations will result in a series of trajectories originating at values of $\bar{y}_0$ which would intersect the surface of the cylinder or pass beyond it. One of these trajectories, originating at $\bar{y}^*$, is tangent to the cylinder, and it is this trajectory which determines the efficiency, $\eta_I = \bar{y}^*/R_c$, of impaction [see fig. 1 from ref. 14].

The efficiency of inertial impaction, η_I, is defined as the ratio of the cross-sectional area of the original aerosol stream from which particle trajectories . . . of a given species and size intersect the surface to the projected area of the collector in the direction of flow.

In order to solve these differential equations, one must examine the flow conditions of a gas across the cylinder. There are two simplified flow conditions that are adequate for a practical solution. One is at high Reynolds numbers ($Re_f \to \infty$) where the flow in front of the cylinder can be considered ideal, inviscid, irrotational, and incompressible, and has the forms of

$$\bar{v}_x = 1 + \frac{\bar{y}^2 - \bar{x}^2}{(\bar{x}^2 + \bar{y}^2)^2} \tag{18}$$

$$\bar{v}_y = \frac{-2\overline{xy}}{(\bar{x}^2 + \bar{y}^2)^2} \tag{19}$$

The other is viscous flow; so far, mathematical solutions for pure viscous flow ($Re_f \to 0$) have not been developed. But when Reynolds numbers are finite, Lamb (ref. 16) has used equations to describe the flow near the cylinder by taking partial account of inertial terms in the differential equations:

$$\bar{v}_x = \frac{1}{2.002 - \ln Re_f} \left[\frac{\ln(\bar{x}^2 + \bar{y}^2)^{1/2} + (\bar{x}^2 + \bar{y}^2 - 1)(\bar{y}^2 - \bar{x}^2)}{2(\bar{x}^2 + \bar{y}^2)^2} \right] \tag{20}$$

$$\bar{v}_y = -\frac{1}{2.002 - \ln Re_f} \left[\frac{(\bar{x}^2 + \bar{y}^2 - 1)\overline{xy}}{(\bar{x}^2 + \bar{y}^2)^2} \right] \tag{21}$$

With different shapes of collectors, however, different equations are needed to describe each flow situation.

To solve equations (16) and (17), which describe the inertial impaction for particles in a free airstream approaching a cylinder, many investigators followed step-by-step calculations starting with the particles at some practical value of $\bar{x}$ ahead of the cylinder. Sell (ref. 7) used his experimentally determined velocity distribution; Albrecht (ref. 8) used equations (18) and (19); Langmuir and Blodgett (ref. 9) used the differential analyzer to establish curves; and Landahl and Herrmann (ref. 10) applied the flow field of Thom (ref. 17). The results of the above investigators, along with the

7

theoretical calculations of Davies (ref. 11) and the experimental results of Wong et al. (ref. 13) are presented here as figure 2 (from ref. 13). These results are examined in detail later in the Discussion section.

So far we have examined the equations that determine particle trajectories resulting from the effects of frictional drag and inertia. We learned that the Knudsen and Reynolds numbers are important to both the air-particle flow field and the air-obstacle flow. In the resulting computations we determined that the inertial parameter ψ provides the mathematical relationship that enables us to determine sampling efficiency for impaction of certain aerosol particles on cylindrical collectors under specified conditions. Finally, we found that controlled laboratory experiments generally confirm theoretical treatments of the flow situations. Therefore, we are now ready to examine our sampling situation to calculate the efficiency corrections needed to accurately depict the particle-size distributions in the stratosphere.

First, however, we notice a striking similarity between the experimental conditions maintained by Wong et al. (ref. 13) in their confirming experiments and our sampling situation in the stratosphere. Wong et al. generated sulfuric acid particles in the size range from 0.56 to 1.40 μm; velocities of their aerosol streams were 3.99 m/sec to 50.90 m/sec; the density of sulfuric acid aerosol was 1.48 g/cm^3; and their platinum collector wires had diameters of 25 μm and 75 μm, their tungsten wires diameters of 50 μm and 100 μm. With those collector diameters and velocities the flow Reynolds numbers had a range from 13 to 330. Their impaction was performed at room temperature and pressure.

In our collection experiments in the stratosphere, the particles consist of a slurry-like fluid (liquid mixed with solid) (ref. 3). Many researchers (refs. 18-22) suggest that the particles are mostly sulfuric acid containing crystalling components, such as ammonium sulfate and volcanic ash. They propose particle densities of about 1.4 g/cm^3. For our study, we chose 1.3 g/cm^3 as an arbitrary value for all calculations; we will justify that choice in a later section. Our collections have been made at altitudes of 12 km to 21 km. Stratospheric particles have sizes ranging from Aitken nuclei (0.01 μm) to a few micrometers and the peak concentrations are of particles of about 0.2 μm (ref. 5). The velocity of the U-2 aircraft at 18 km is about 200 m/sec. Collectors are 25-μm and 75-μm palladium wires. The flow Reynolds numbers based on these wire diameters for these conditions are about 42 and 127, respectively, within the experimental range of Wong et al. The temperature ranges from -40° to -60° C; pressures and viscosities are those at sampling altitudes. By using the Cunningham correction factors to account for different altitudes, our sampling conditions are in many ways almost a duplication of those of the Wong et al. study. Consequently, our use of their derived curve of inertial parameters vs efficiency is justified.

APPLICATION

The following is an example of the method we use to calculate collection efficiency for stratospheric particles on 75-μm-diam wires at an altitude of 18 km.

Let us restate the inertial impaction parameter equation

$$\psi^{1/2} = \left(\frac{C_c \rho_i v}{18 \mu_g D_c}\right)^{1/2} D_p \tag{22}$$

and

$$C_c = 1 + \frac{2\lambda_g}{D_p}\left[1.23 + 0.41 \exp\left(-0.44 \frac{D_p}{\lambda_g}\right)\right] .$$

where

ψ inertial impaction parameter

C_c Cunningham slip factor

ρ_i density of particle

v airstream velocity, or collector velocity

μ_g viscosity of fluid

D_c collector diameter

λ_g mean free path of air molecules

Values for the variables at 18 km are

$$\rho_i = 1.3 \times 10^3 \text{ kg/m}^3$$

$$v = 205.78 \text{ m/sec}$$

$$\mu_g = 1.4216 \times 10^{-5} \text{ kg/msec}$$

$$D_c = 7.5 \times 10^{-5} \text{ m}$$

$$\lambda_g = 6.9883 \times 10^{-7} \text{ m}$$

$$D_p = 0.1 \text{ }\mu m \text{ or } 10^{-7} \text{ m}$$

Substituting the given values into the inertial impaction parameter and the Cunningham slip factor equation, we get

$$\psi^{1/2} = 1.8127$$

Now, using the experimental curve of Wong et al. vs impaction efficiency (fig. 2) we obtain a collection efficiency of 89% for a particle of this small size. Thus, when we count the number of such particles on our collectors, we

must increase that count by the ratio 100%:89% to obtain the actual strato-spheric population of that size.

To investigate the collection efficiency of 75-μm and 25-μm wires for all particle sizes and altitudes of interest (from 9 km to 21 km), we selected nine altitudes separated by 1.5 km. For each altitude and collector diameter, we calculated the impaction parameters for particle sizes from 0.01 μm, in 0.01 μm intervals, up to a particle size that gave the $\sqrt{\psi}$ value of 100% efficiency on the Wong et al. experimental curve (fig. 2). These impaction parameters thus gave us collection efficiencies for each particle size and altitude (see figs. 3 and 4). Reconstructing these, we obtained the particle size vs collection efficiency curves shown in figures 5 and 6. We also arranged these efficiency values in tabular form (see tables 1 and 2) for computer storage to enable correction of future sample counts.

As we stated before, we assume the Reynolds number in the gas-particle system Re_i is <0.1 in our sampling situation and it need not be considered further here. However, to properly use the Wong et al. curve in figure 2, the flow Reynolds number (Re_f) should be in the range of 13 to 330. As an example, we calculate the Re_f for our collector at 18 km as follows:

$$Re_f = \frac{D_c v}{\nu_f} \tag{23}$$

where

ν_f kinematic viscosity $= \dfrac{\mu_g}{\rho_g}$

D_c 7.5×10^{-5} m (3-mil wire)

v 205.78 m/sec

ν_f 1.2196×10^{-4} m^2/sec at 18 km

Substituting these values in equation (23) gives $Re_f = 127$. Thus, we demonstrate that our sampling situation at 18 km conforms to the requirements of Wong et al. (fig. 2). Because the kinematic viscosity changes with altitude, we have different Reynolds numbers of flow for our collector diameter at different altitudes; but these Reynolds numbers are all within the required range.

DISCUSSION

If we compare all the theoretical results, we find that they are not in good agreement, but generally follow an S-shape curve, except the calculation of Davies (ref. 11) with a flow Reynolds number of 0.2. The experimental results of Wong et al. for Reynolds numbers ranging from $13 < Re_f < 330$ closely agree with those by Langmuir and Blodgett for potential flow and those by Landahl and Herrmann for a Reynolds number of 10 at $\sqrt{\psi}$ value below 1.4;

however, the experimental values are higher for values of $\sqrt{\psi}$ greater than 1.4. As we have shown, our collection and flow conditions are about the same as the experimental conditions of Wong et al., except for pressure, which is correctable by the Cunningham slip factor in the inertial impaction parameter equation. For all of the above reasons it is more appropriate for us to apply the results of Wong et al. than the results of others.

We have stated that the particle density value we chose was slightly different from that used by other experimenters. We selected this density based on the work of Farlow et al. (ref. 5) in which they found that the composition of stratospheric aerosols is perhaps more dilute than the 75% H_2SO_4 proposed by others. For example, the density of 75% sulfuric acid is about 1.4 g/cm^3, while the more dilute mix of acid and crystals suggested by Farlow et al. is nearer 1.3 g/cm^3.

Particle shape can significantly influence inertial impaction calculations because of varying drag forces in air. In nature, most solid aerosol particles are nonspherical; on the other hand, liquid particles are spherical. Nonspherical particles behave quite differently from the spherical ones when falling through a resistant medium; the direction of fall of nonspherical particles can deviate significantly from a vertical path. Since aerosol particles are liquid-like in the stratosphere, we reasonably assume they are spherical for our calculations.

We have said that aerosol collection is influenced by mechanisms other than inertial impaction, such as Brownian diffusion, electrical forces, gravity settling, thermal force, and direct interception. After examining these mechanisms in detail we have found them to be insignificant under the collection conditions we have described; confirming calculations are presented in the appendix.

CONCLUSION

With the methods described in this paper, we are able to determine the collection efficiencies of our wire collectors for particles of all sizes at the altitudes of interest. With these we can correct the measured size-frequency curves to reflect the actual particle populations in the stratosphere. We use figures 5 and 6 and tables 1 and 2 to obtain the necessary corrections. The mathematical considerations presented in this paper show that aerosol particles of all sizes found in the stratosphere are collectible by our wire impaction technique with efficiencies that permit reliable computations of the actual populations.

There is, however, an unresolved problem. The experiments of Wong et al. (ref. 13) represented collections analyzed as total collections across the whole wire diameter. Langmuir and Blodgett (ref. 9) had shown theoretically that the local collection efficiency at the stagnation point directly facing into the airstream could be more efficient (by perhaps 15%) than the wire as a whole. This has not been tested experimentally. Our particle sizing

11

methods (ref. 5), however, use observations at the wire stagnation point. Thus, our actual collection efficiencies may be somewhat higher than the corrections we apply. Although our present corrections are conservative, we intend to construct a stagnation point correction. We will do this by analyzing several collections both at the stagnation point and across the whole wire diameter. From these data we will determine factors that represent the improved efficiency at the stagnation point for each particle size. These factors will then be applied as a correction to the efficiency curve of Wong et al. and subsequently to our stagnation point size distributions.

APPENDIX

INSIGNIFICANT EFFECTS OF CERTAIN MECHANISMS

ON AEROSOL COLLECTION

Collection by Brownian diffusion occurs when small particles in random motion deviate from the air streamlines to contact and adhere to the collector surface. Stairmand (ref. 23) has derived an equation of Brownian diffusion collection efficiency for potential flow that represents the proportion of small particles that will be collected by this mechanism:

$$E_D = 2.83 \frac{1}{Pe^{1/2}} \tag{24}$$

where

Pe   Peclet number, $D_c \frac{v}{D}$

D_c collector diameter

D $\frac{C_c KT}{3\pi\mu_g D_p}$

v   gas velocity

D   Brownian coefficient

C_c Cunningham slip factor

K   Boltzmann's constant

T   absolute temperature

μ_g viscosity of gas

D_p particle diameter

For $D_c = 7.5\times10^{-5}$ m, $D_p = 10^{-8}$ m, v = 204.78 m/sec, $\mu_g = 1.4216\times10^{-5}$ kg/msec, T = 223 K, K = 1.38×10^{-23} J/K, then D = 5.28×10^{-7} m^2/sec; Pe = 2.92×10^4; and E_D = 0.017.

For viscous flow, Johnstone and Roberts (ref. 24) and Ranz (ref. 25) suggested the following relation for Brownian diffusion efficiency:

$$E_D = \frac{1}{Pe} + 1.727 \frac{Re_f^{1/6}}{Pe^{2/3}} \tag{25}$$

13

where Re_f is Reynolds number of flow. Given $Re_f = 127$, $Pe = 2.92 \times 10^4$, as in potential flow calculations, then

$$E_D = 4.12 \times 10^{-3}$$

We see from the above values for both potential and viscous flow regime that the collection efficiency contributed by Brownian diffusion is small.

Deposition of particles by electrostatic force is practically nil due to the fact that our collection device does not charge up the particles and the wire, and has no voltage differential between the wire and the module case.

Thermal precipitation of particles would be significant only if the aerosol stream passed through a thermal gradient, such as between a hot and a cold collection plate. Thermal forces then could drive the particles toward the cold surface. However, that is not the case in our collection configuration.

Gravity settling of aerosol particles as the stream flows past the collector is also not important as shown by the following calculations from the formula derived by Ranz (ref. 25), where E_G = proportion of particles that will be collected by gravitational settling.

$$E_G = \frac{v_s}{v} \tag{26}$$

where v_s = stationary sedimentation velocity of particles and v = velocity of gas. But,

$$v_s = \tau g$$

where τ = relaxation time, $C_c \rho_i D_p^2 / 18 \mu_g$, and g = gravity acceleration (9.7504 m/sec^2 at 18 km), and

$$v_s = \frac{C_c \rho_g D_p^2}{18 \mu_g} \times g$$

When $C_c = 229.8566$, $\rho_i = 1.3 \times 10^3$ kg/m^3, $D_p = 10^{-5}$ m, $\mu_g = 1.4216 \times 10^{-5}$ kg/msec, $v_s = 1.14$ m/sec, and $v = 205.78$ m/sec, then $E_G = 0.0055$.

For 10-μm particles and smaller it is clear that collection by gravity settling is negligible. In the stratosphere, most particles are smaller than this size.

Direct particle interception occurs when a particle follows the gas streamline around the wire and is collected wherever its trajectory approaches within a distance of $D_p/2$ of the collector surface. Direct interception is described by the parameter

14

$$N_R = \frac{D_p}{D_c} \qquad (27)$$

where D_p = particle diameter and D_c = collector diameter.

For potential flow, the proportion of particles collected by direct interception is calculated with the following equation (ref. 26):

$$E_R = 1 + N_R - \frac{1}{1 + N_R} \qquad (28)$$

In the stratosphere when the median particle size (D_p) is near 0.2 μm (2×10^{-7} m), $D_c = 7.5 \times 10^{-5}$ m, and $N_R = 2.67 \times 10^{-3}$, then the interception efficiency (E_R) is 0.0054. This very low value clearly shows that collection by this mechanism is negligible.

Conclusively, inertial impaction is the only significant effect causing deposition of aerosols on our sampling system at stratospheric conditions.

REFERENCES

1. Ferry, G. V.; and Lem, H. Y.: Aerosols at 20 Kilometers Altitude. Proc. of the Second International Conference on the Environmental Impact of Aerospace Operations in the High Atmosphere, American Meteorological Society, Boston, Mass., 1974.

2. Farlow, N. H.; Ferry, G. V.; and Lem, H. Y.: Analysis of Individual Particles Collected from the Stratosphere. Space Res., vol. XIII, 1973, pp. 1153-1157.

3. Farlow, N. H.; Hayes, D. M.; and Lem, H. Y.: Stratospheric Aerosols: Undissolved Granules and Physical State. J. Geophys. Res., vol. 82, 1977, pp. 4921-4927.

4. Farlow, N. H.; Snetsinger, K. G.; Hayes, D. M.; Lem, H. Y.; and Tooper, B. M.: Nitrogen-Sulphur Compounds in Stratospheric Aerosols. J. Geophys. Res., vol. 83, 1978, pp. 6027-6211.

5. Farlow, N. H.; Ferry, G. V.; Lem, H. Y.; and Hayes, D. M.: Latitudinal Variations of Stratospheric Aerosols. J. Geophys. Res., vol. 84, 1979, pp. 733-742.

6. Ferry, G. V.; and Lem, H. Y.: Aerosols in the Stratosphere. Proc. of the Third Conference of the Climatic Assessment Program, Rep. DOT-TSC-OST-74-15, Department of Transportation, Washington, D.C., 1974.

7. Sell, W.: Dust Precipitation on Simple Bodies and in Air Filters. Forsch. Gebiete Ingenieurw. 2, Forschungsheft 347, 1931, pp. 1-22.

8. Albrecht, F.: Theoretical Investigation of Dust Deposition from Flowing Air and Its Application to the Theory of the Dust Filter. Physik. Zeits., vol. 32, 1931, pp. 48-56.

9. Langmuir, I.; and Blodgett, K. B.: Mathematical Investigation of Water Droplet Trajectories. G. E. C. Res. Lab. Schenectady, N.Y. Report RL 225, 1944-1945.

10. Landahl, H. D.; and Herrmann, R. G.: Sampling of Liquid Aerosols by Wires, Cylinders, and Slides, and the Efficiency of Impaction of the Droplets. J. Colloid. Sci., vol. 4, 1949, pp. 103-136.

11. Davies, C. N.: Separation of Airborne Dust and Particles. Proc. Inst. Mech. Engrs. (London) B1, 1952, pp. 185-198, Discussion pp. 199-213.

12. Ranz, W. E.; and Wong, J. B.: Impaction of Dust and Smoke Particles on Surfaces and Body Collectors. Industrial Engineering Chemistry, vol. 44, 1952, pp. 1371-1381.

13. Wong, J. B.; Ranz, W. E.; and Johnstone, H. F.: Inertial Impaction of Aerosol Particles on Cylinders. J. Appl. Physics, vol. 26, 1955, pp. 244-249.

14. Hidy, G. M.; and Brock, J. R.: International Reviews in Aerosol Physics and Chemistry. Vol. 1. Pergamon Press (Oxford), 1970.

15. Davies, C. N.: Aerosol Science. Theory of Aerosol Filtration by Fibrous and Membrane Filter. J. Pich, ed., Academic Press, Inc., 1966, pp. 223-285.

16. Lamb, H.: Hydrodynamics. Sixth ed. Cambridge University Press (Cambridge), 1932.

17. Thom, A.: Flow Past Circular Cylinders at Low Speeds. Proc. of Royal Society (London), vol. 141A, 1933, pp. 651-669.

18. Rosen, J. M.: The Boiling Point of Stratospheric Aerosols. J. Appl. Meteorol., vol. 10, 1971, pp. 1044-1045.

19. Junge, C. E.; and Manson, J. E.: Stratospheric Aerosol Studies. J. Geophys. Res., vol. 66, 1961, pp. 2163-2182.

20. Junge, C. E.: Air Chemistry and Radioactivity. Academic Press, Inc., 1963, pp. 196.

21. Mossop, S. C.: Stratospheric Particles at 20 km Altitude. Geochim. Cosmochim. Acta, vol. 29, 1965, pp. 201-207.

22. Bigg, E. K.: Stratospheric Particles. J. Atmos. Sci., vol. 32, 1975, pp. 910-917.

23. Stairmand, C. J.: Dust Collection by Impingement and Diffusion. Trans. Inst. Chem. Engrs. (London), vol. 28, 1950, pp. 130-139.

24. Johnstone, H. F.; and Roberts, M. H.: Deposition of Aerosol Particles from Moving Gas Streams. Ind. Engng. Chem., vol. 41, 1949, pp. 2417-2423.

25. Ranz, W. E.: The Impaction of Aerosol Particles on Cylindrical and Spherical Collectors. Tech. Report No. 3, Contract AT-(30-3)-28, University of Illinois, 1951.

26. Fuchs, H. A. (Daisley, R. E.; and Fuchs, M., transl.): The Mechanics of Aerosols. Pergamon Press, 1964.

$D_p{}^a$	Altitude, km									$D_p{}^a$
	9.1	10.7	12.2	13.7	15.2	16.8	18.3	19.8	21.3	
0.63	1.000	1.000	1.000	1.000	1.000	1.000	1.000	1.000	1.000	0.63
.62	.998	1.000	1.000	1.000	1.000	1.000	1.000	1.000	1.000	.62
.61	.995	1.000	1.000	1.000	1.000	1.000	1.000	1.000	1.000	.61
.60	.992	1.000	1.000	1.000	1.000	1.000	1.000	1.000	1.000	.60
.59	.988	1.000	1.000	1.000	1.000	1.000	1.000	1.000	1.000	.59
.58	.984	1.000	1.000	1.000	1.000	1.000	1.000	1.000	1.000	.58
.57	.979	1.000	1.000	1.000	1.000	1.000	1.000	1.000	1.000	.57
.56	.974	1.000	1.000	1.000	1.000	1.000	1.000	1.000	1.000	.56
.55	.970	1.000	1.000	1.000	1.000	1.000	1.000	1.000	1.000	.55
.54	.965	1.000	1.000	1.000	1.000	1.000	1.000	1.000	1.000	.54
.53	.960	.997	1.000	1.000	1.000	1.000	1.000	1.000	1.000	.53
.52	.954	.995	1.000	1.000	1.000	1.000	1.000	1.000	1.000	.52
.51	.949	.992	1.000	1.000	1.000	1.000	1.000	1.000	1.000	.51
.50	.943	.988	1.000	.000	1.000	1.000	1.000	1.000	1.000	.50
.49	.935	.983	1.000	1.000	1.000	1.000	1.000	1.000	1.000	.49
.48	.929	.978	1.000	1.000	1.000	1.000	1.000	1.000	1.000	.48
.47	.924	.973	1.000	1.000	1.000	1.000	1.000	1.000	1.000	.47
.46	.915	.967	1.000	1.000	1.000	1.000	1.000	1.000	1.000	.46
.45	.908	.963	1.000	1.000	1.000	1.000	1.000	1.000	1.000	.45
.44	.899	.957	.999	1.000	1.000	1.000	1.000	1.000	1.000	.44
.43	.890	.952	.995	1.000	1.000	1.000	1.000	1.000	1.000	.43
.42	.881	.944	.991	1.000	1.000	1.000	1.000	1.000	1.000	.42
.41	.871	.938	.987	1.000	1.000	1.000	1.000	1.000	1.000	.41
.40	.862	.930	.983	1.000	1.000	1.000	1.000	1.000	1.000	.40
.39	.852	.922	.978	1.000	1.000	1.000	1.000	1.000	1.000	.39
.38	.842	.914	.972	1.000	1.000	1.000	1.000	1.000	1.000	.38
.37	.831	.904	.966	1.000	1.000	1.000	1.000	1.000	1.000	.37
.36	.820	.896	.960	1.000	1.000	1.000	1.000	1.000	1.000	.36
.35	.808	.886	.954	1.000	1.000	1.000	1.000	1.000	1.000	.35
.34	.795	.875	.946	.995	1.000	1.000	1.000	1.000	1.000	.34
.33	.783	.864	.938	.991	1.000	1.000	1.000	1.000	1.000	.33
.32	.769	.853	.930	.985	1.000	1.000	1.000	1.000	1.000	.32
.31	.755	.838	.922	.979	1.000	1.000	1.000	1.000	1.000	.31
.30	.742	.827	.911	.972	1.000	1.000	1.000	1.000	1.000	.30
.29	.727	.814	.900	.965	1.000	1.000	1.000	1.000	1.000	.29
.28	.712	.800	.889	.958	1.000	1.000	1.000	1.000	1.000	.28
.27	.696	.786	.877	.950	1.000	1.000	1.000	1.000	1.000	.27
.26	.680	.770	.864	.942	1.000	1.000	1.000	1.000	1.000	.26
.25	.663	.755	.850	.931	.994	1.000	1.000	1.000	1.000	.25
.24	.644	.740	.836	.920	.986	1.000	1.000	1.000	1.000	.24
.23	.627	.723	.822	.907	.979	1.000	1.000	1.000	1.000	.23
.22	.606	.704	.805	.895	.970	1.000	1.000	1.000	1.000	.22
.21	.585	.685	.788	.881	.962	.997	1.000	1.000	1.000	.21

TABLE 1.- CONCLUDED

$D_p{}^a$	Altitude, km									$D_p{}^a$
	9.1	10.7	12.2	13.7	15.2	16.8	18.3	19.8	21.3	
0.20	0.563	0.666	0.770	0.865	0.950	0.988	1.000	1.000	1.000	0.20
.19	.542	.644	.751	.848	.938	.981	1.000	1.000	1.000	.19
.18	.517	.622	.730	.831	.924	.971	1.000	1.000	1.000	.18
.17	.494	.599	.708	.810	.911	.960	.998	1.000	1.000	.17
.16	.475	.575	.684	.788	.894	.947	.988	1.000	1.000	.16
.15	.437	.546	.658	.766	.875	.933	.977	1.000	1.000	.15
.14	.407	.519	.632	.741	.854	.914	.965	1.000	1.000	.14
.13	.377	.488	.603	.714	.830	.895	.949	.991	1.000	.13
.12	.342	.457	.572	.685	.804	.872	.932	.977	1.000	.12
.11	.305	.422	.539	.655	.775	.846	.911	.962	1.000	.11
.10	.266	.383	.501	.618	.743	.816	.885	.942	.985	.10
.09	.226	.342	.460	.579	.706	.782	.854	.915	.967	.09
.08	.184	.296	.413	.536	.664	.745	.815	.884	.943	.08
.07	.148	.246	.360	.485	.615	.698	.772	.846	.912	.07
.06	.114	.195	.300	.427	.558	.644	.722	.799	.871	.06
.05	.082	.142	.234	.357	.487	.580	.658	.740	.816	.05
.04	.052	.095	.167	.272	.405	.497	.578	.665	.744	.04
.03	.030	.057	.103	.174	.299	.387	.473	.564	.647	.03
.02	.010	.023	.048	.078	.170	.237	.323	.408	.499	.02
.01	.000	.003	.009	.023	.053	.079	.105	.166	.243	.01

$a D_p$ = particle diameter, μm

TABLE 2.- FRACTIONAL EFFICIENCY OF INERTIAL
IMPACTION: COLLECTOR DIAMETER = 25 μm

$D_p{}^a$	Altitude, km									$D_p{}^a$
	9.1	10.7	12.2	13.7	15.2	16.8	18.3	19.8	21.3	
0.29	1.000	1.000	1.000	1.000	1.000	1.000	1.000	1.000	1.000	0.29
.28	.997	1.000	1.000	1.000	1.000	1.000	1.000	1.000	1.000	.28
.27	.990	1.000	1.000	1.000	1.000	1.000	1.000	1.000	1.000	.27
.26	.983	1.000	1.000	1.000	1.000	1.000	1.000	1.000	1.000	.26
.25	.975	1.000	1.000	1.000	1.000	1.000	1.000	1.000	1.000	.25
.24	.963	1.000	1.000	1.000	1.000	1.000	1.000	1.000	1.000	.24
.23	.955	1.000	1.000	1.000	1.000	1.000	1.000	1.000	1.000	.23
.22	.944	.996	1.000	1.000	1.000	1.000	1.000	1.000	1.000	.22
.21	.933	.987	1.000	1.000	1.000	1.000	1.000	1.000	1.000	.21
.20	.918	.978	1.000	1.000	1.000	1.000	1.000	1.000	1.000	.20
.19	.901	.967	1.000	1.000	1.000	1.000	1.000	1.000	1.000	.19
.18	.884	.956	1.000	1.000	1.000	1.000	1.000	1.000	1.000	.18
.17	.865	.940	.996	1.000	1.000	1.000	1.000	1.000	1.000	.17
.16	.843	.925	.985	1.000	1.000	1.000	1.000	1.000	1.000	.16
.15	.820	.907	.974	1.000	1.000	1.000	1.000	1.000	1.000	.15
.14	.797	.886	.959	1.000	1.000	1.000	1.000	1.000	1.000	.14
.13	.768	.864	.943	.999	1.000	1.000	1.000	1.000	1.000	.13
.12	.738	.838	.924	.986	1.000	1.000	1.000	1.000	1.000	.12
.11	.704	.806	.900	.972	1.000	1.000	1.000	1.000	1.000	.11
.10	.667	.775	.872	.954	1.000	1.000	1.000	1.000	1.000	.10
.09	.627	.736	.838	.929	.995	1.000	1.000	1.000	1.000	.09
.08	.580	.692	.799	.898	.975	1.000	1.000	1.000	1.000	.08
.07	.530	.642	.754	.859	.949	.990	1.000	1.000	1.000	.07
.06	.469	.584	.698	.812	.914	.962	1.000	1.000	1.000	.06
.05	.398	.515	.634	.752	.864	.923	.974	1.000	1.000	.05
.04	.310	.430	.550	.676	.796	.866	.928	.976	1.000	.04
.03	.206	.310	.443	.569	.699	.776	.852	.910	.968	.03
.02	.103	.183	.295	.417	.552	.637	.722	.797	.870	.02
.01	.027	.053	.101	.174	.293	.383	.475	.562	.643	.01

$^a D_p$ = particle diameter, μm

STREAMLINES

$z' = r$

x'

θ

A

V

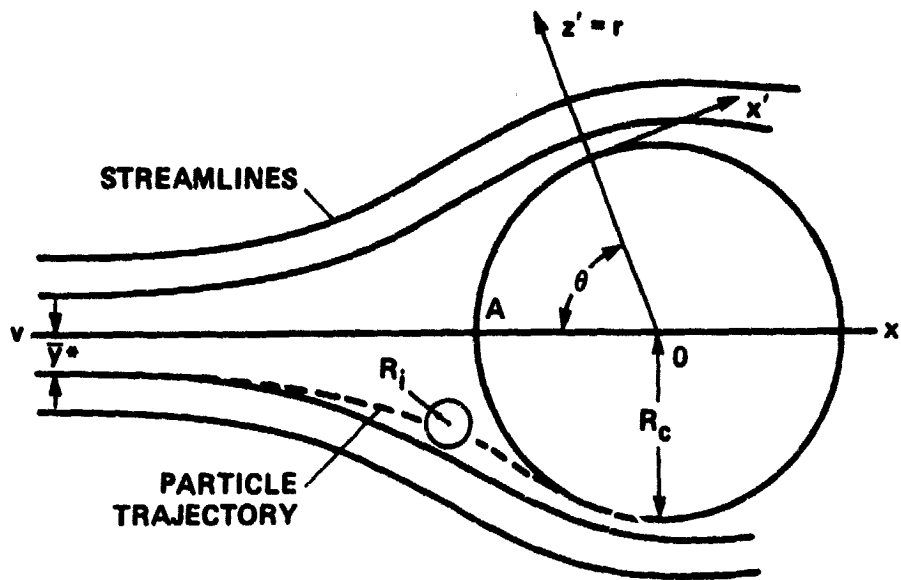$\bar{y}*$

R_i

R_c

O

x

PARTICLE
TRAJECTORY

Figure 1.- Diagram of a particle trajectory approaching an infinitely long
cylinder placed in a uniform flow.

– – – – – – Sell's theory (ref. 7) based on experimental flowlines (high Re_f)

— – – — Albrecht's theory (ref. 8) based on potential flow (high Re_f)

— — — Langmuir and Blodgett theory (ref. 9) based on potential flow (high Re_f)

— · — · — Landahl and Herrmann theory (ref. 10) based on Thom's calculated flowlines ($Re_f = 10$)

———— Davies' theory (ref. 11) based on viscous flow ($Re_f = 0.2$)
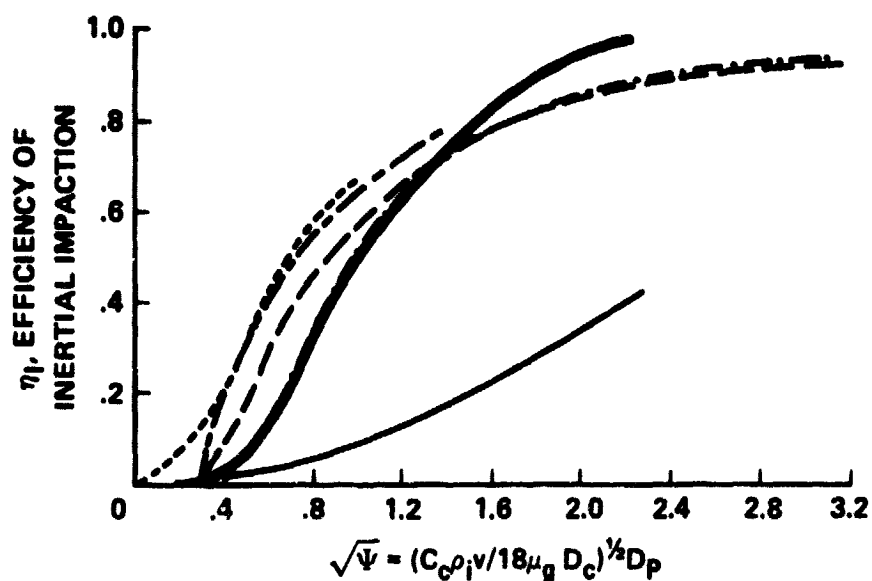
━━━━ Experimental ($13 < Re_f < 330$)

Figure 2.- Comparison of theoretical and experimental efficiencies of inertial impaction on circular cylinders.

Collector diameter (Cylinder) = 75 μm

η_i EFFICIENCY OF INERTIAL IMPACTION

$$Re_f = \frac{D_c v}{\mu_i}$$

$Re_f = 304$ at 9.1 km
$Re_f = 291$ at 10.7 km
$Re_f = 258$ at 12.2 km
$Re_f = 227$ at 13.7 km
$Re_f = 204$ at 15.2 km
$Re_f = 161$ at 16.8 km
$Re_f = 127$ at 18.3 km
$Re_f = 100$ at 19.8 km
$Re_f = 78$ at 21.3 km

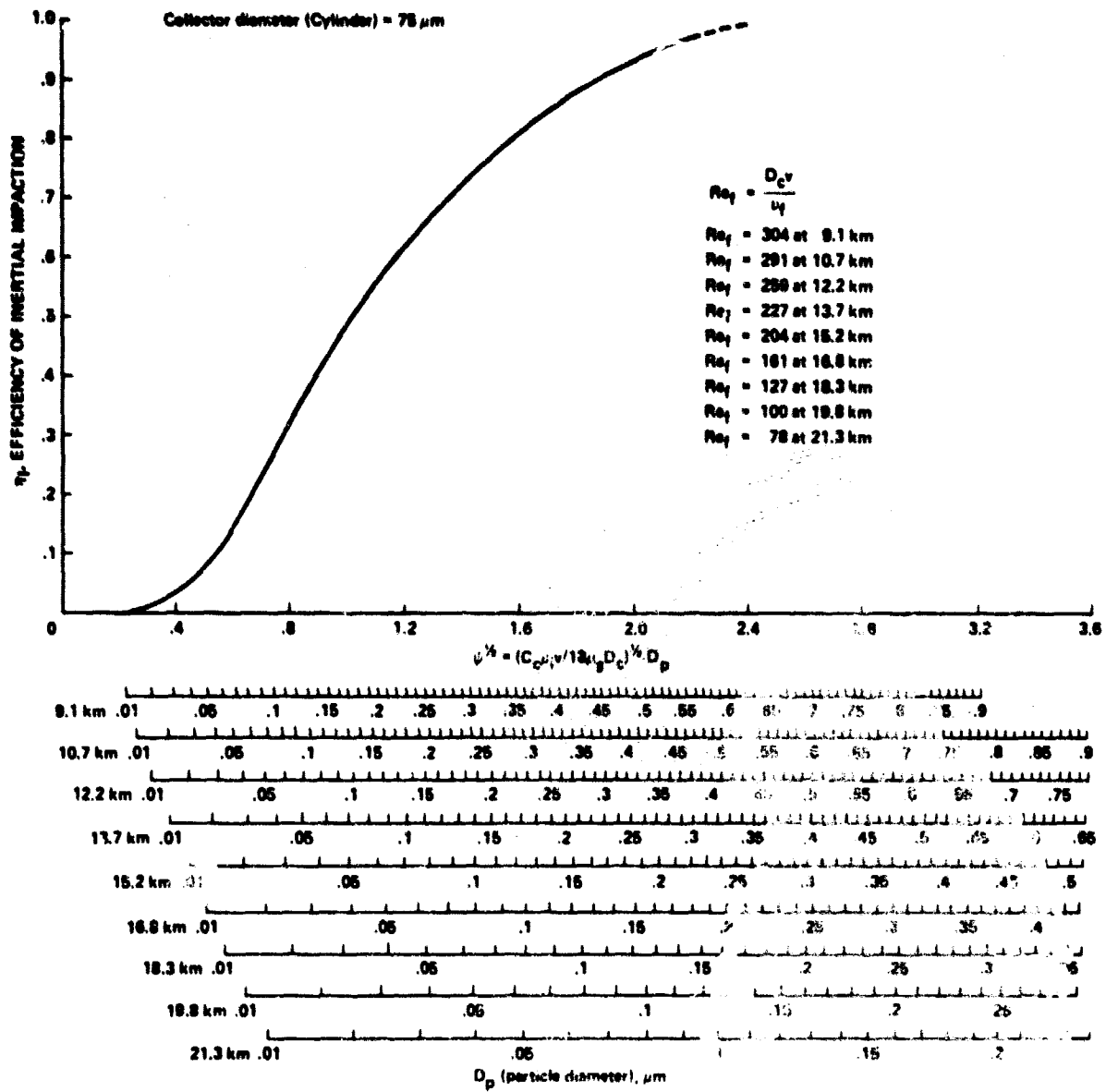$\psi^{1/2} = (C_c \mu_i v / 18 \mu_g D_c)^{1/2} D_p$

D_p (particle diameter), μm

Figure 3.- Collection efficiency of a 75-μm-diam cylinder for various particle sizes at different altitudes and inertial parameter values.

23

Collector diameter (Cylinder) = 25 μm

η, EFFICIENCY OF INERTIAL IMPACTION

$$\eta_q = \frac{D_c v}{\nu}$$

$Re_q = 101$ at 9.1 km
$Re_q = 97$ at 10.7 km
$Re_q = 86$ at 12.2 km
$Re_q = 76$ at 13.7 km
$Re_q = 66$ at 15.2 km
$Re_q = 54$ at 16.8 km
$Re_q = 42$ at 18.3 km
$Re_q = 33$ at 19.8 km
$Re_q = 26$ at 21.3 km

1.0
.9
.8
.7
.6
.5
.4
.3
.2

0   .4   .8   1.2   1.6   2.0   2.4   2.8   3.2   3.6

$$\psi^{1/2} = (C_c \rho_f v / 18 \mu_g D_c)^{1/2} D_p$$

9.1 km .01   .05   .1   .15   .2   .25   .3   .35   .4   .45   .5
10.7 km .01   .05   .1   .15   .2   .25   .3   .35   .4
12.2 km .01   .05   .1   .15   .2   .25   .7
13.7 km .01   .05   .1   .15   .2   .25
15.2 km .01   .05   .1   .15
16.8 km .01   .05   .1   .15
18.3 km .01   .05   .1
19.8 km .01   .05   .1
21.3 km .01   .05

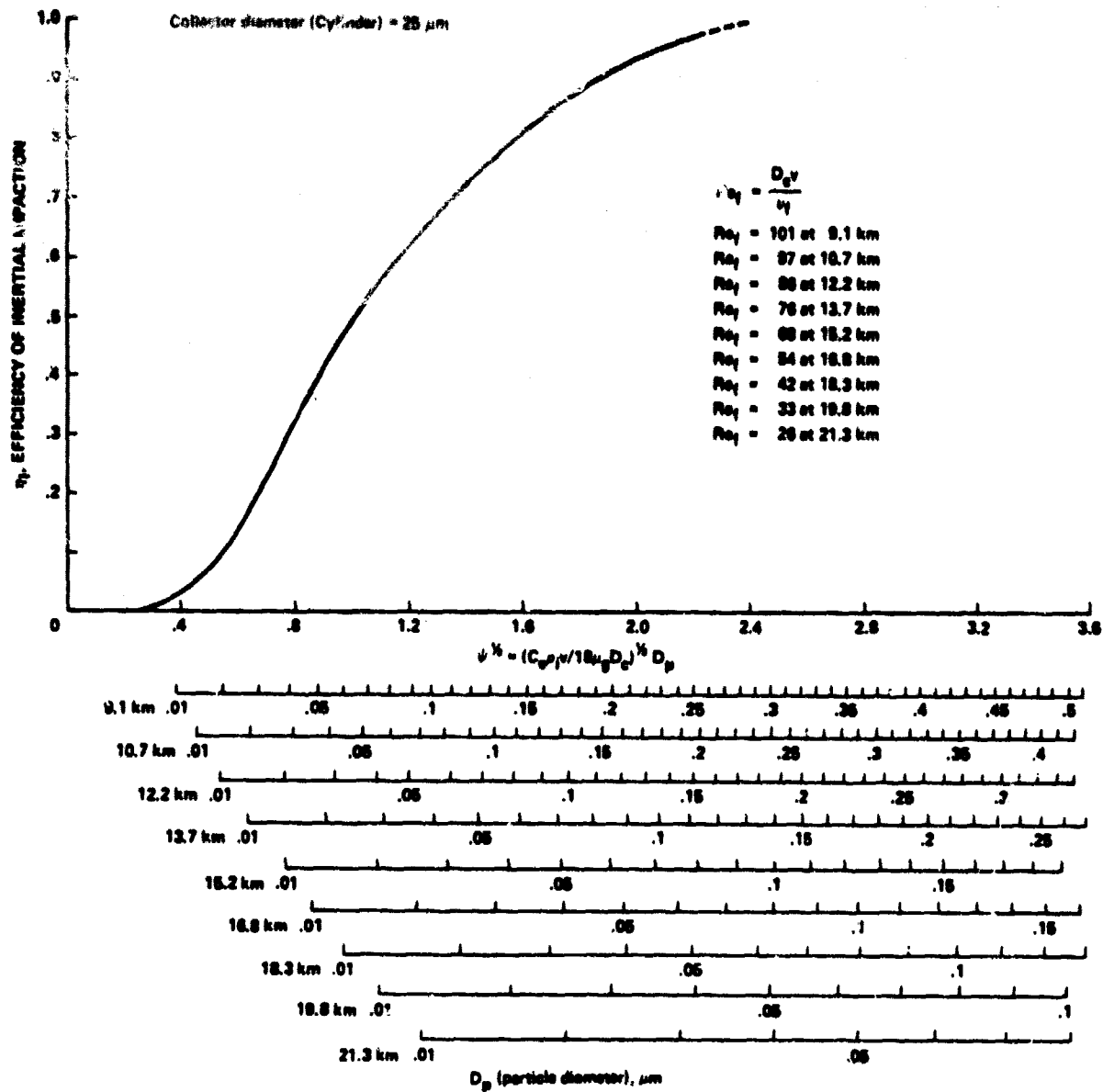D_p (particle diameter), μm

Figure 4.- Collection efficiency of a 25-μm-diam cylinder for various particle
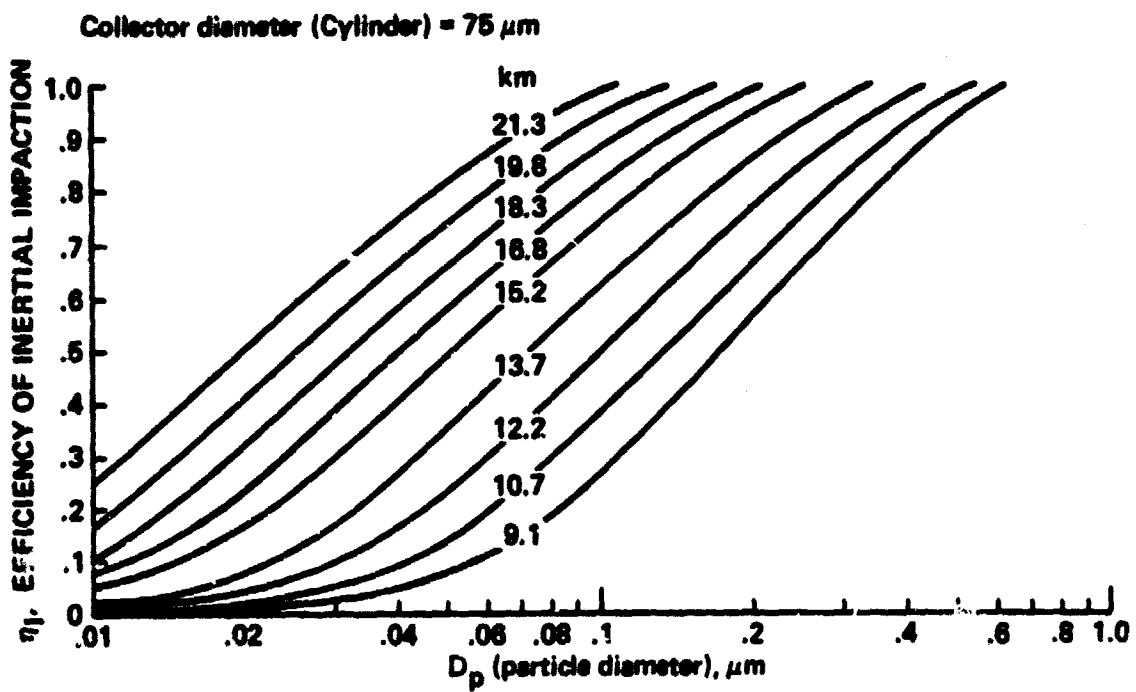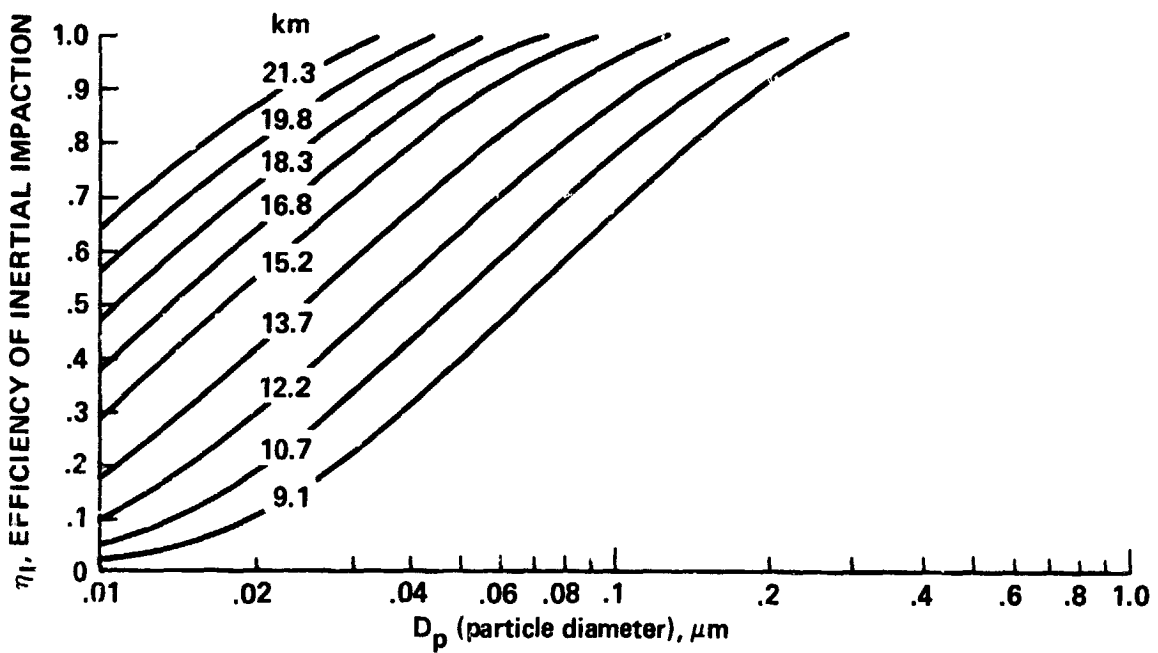sizes at different altitudes and inertial parameter values.

24

Figure 5.- Collection efficiency of a 75-μm-diam cylinder for various particle sizes at different altitudes.

Collector diameter (Cylinder) = 25 μm

Figure 6.- Collection efficiency of a 25-μm-diam cylinder for various particle sizes at different altitudes.